

1

2

3 **Seed hemicelluloses tailor mucilage properties and salt tolerance**

4

5 Bo Yang^{1,2}, Florian Hofmann^{1,3}, Björn Usadel^{1,3,4}, Cătălin Voiniciuc^{1,2,3}

6

7 ¹Institute for Botany and Molecular Genetics (IBMG), BioSC, RWTH Aachen University, 52074
8 Aachen, Germany; ²Independent Junior Research Group–Designer Glycans, Leibniz Institute of
9 Plant Biochemistry, 06120 Halle (Saale), Germany; ³Institute for Bio- and Geosciences (IBG-2:
10 Plant Sciences), Forschungszentrum Jülich, 52425 Jülich, Germany;

11

12 ⁴Present addresses: Institute for Bio- and Geosciences (IBG-4: Bioinformatics),
13 Forschungszentrum Jülich, 52425 Jülich, Germany; and Institute for Biological Data Science,
14 Heinrich Heine University, 40225 Düsseldorf, Germany;

15

16 Author for correspondence:

17 Cătălin Voiniciuc

18 Tel: +49 345 5582 1720

19 Email: catalin.voiniciuc@ipb-halle.de

20

21

22

23

24 **Key words:** germination, glycosyltransferase, hemicellulose, salinity, seed mucilage

25

26

27 **E-Mails and ORCID**

B.Y.	bo.yang@ipb-halle.de	0000-0003-4446-0415
F.H.	f.hofmann35@gmail.com	
B.U.	b.usadel@fz-juelich.de	0000-0003-0921-8041
C.V.	catalin.voiniciuc@ipb-halle.de	0000-0001-9105-014X

28

29

30 **Summary**

- 31 • While *Arabidopsis* seed coat epidermal cells have become an excellent genetic system to
32 study the biosynthesis and structural roles of various cell wall polymers, the
33 physiological function of the secreted mucilaginous polysaccharides remains ambiguous.
34 Seed mucilage is shaped by two distinct classes of highly substituted hemicelluloses
35 along with cellulose and structural proteins, but their interplay has not been explored.
- 36 • We deciphered the functions of four distinct classes of cell wall polymers by generating a
37 series of double mutants with defects in heteromannan, xylan, cellulose, or the
38 arabinogalactan protein SALT-OVERLY SENSITIVE 5 (SOS5), and evaluating their
39 impact on mucilage architecture and on seed germination during salt stress.
- 40 • We discovered that *muci10* seeds, lacking heteromannan branches, had elevated tolerance
41 to salt stress, while heteromannan elongation mutants exhibited reduced germination in
42 CaCl₂. In contrast, xylan made by *MUCILAGE-RELATED21* (*MUCI21*) was found to be
43 required for the adherence of mucilage pectin to microfibrils made by CELLULOSE
44 SYNTHASE5 (*CESA5*) as well as to a SOS5-mediated network.
- 45 • Our results indicate that the substitution of xylan and glucomannan in seeds can fine-tune
46 mucilage adherence and salt tolerance, respectively. The study of germinating seeds can
47 thus provide insights into the synthesis, modification and function of complex glycans.

49 **Introduction**

50 Cellulose microfibrils are deposited around plant cells and enmeshed in a complex matrix of
51 hemicelluloses, pectin, and, to a lesser extent, structural proteins. The roles of specific classes of
52 cell wall polymers have been difficult to study even in model organisms. For instance,
53 *Arabidopsis thaliana* has nine *CELLULOSE SYNTHASE-LIKE A* (*CSLA*) genes that are at least
54 putatively involved in the synthesis of heteromannan (HM), a class of hemicellulose mainly built
55 of β -1,4-linked mannosyl units. While HM polymers could store carbon to feed growing
56 seedlings or directly control cell wall structure (Schröder *et al.*, 2009), their physiological roles
57 in *Arabidopsis* are poorly understood. Genetic disruption of *CSLA7* is embryo-lethal, but *csla2*
58 *csla3 csla9* triple mutant stems had no phenotypic changes despite lacking detectable HM
59 (Goubet *et al.*, 2009). Significant insights into the biosynthesis and functions of various cell wall

60 components, including HM, have been gained using the Arabidopsis seed coat as a genetic model
61 (Šola *et al.*, 2019). The seed coat epidermis secretes large amounts of polysaccharides that
62 rapidly swell upon hydration to release non-adherent mucilage as well as an adherent capsule.
63 Unbranched pectin is the dominant mucilage component, but the adherent capsule also contains
64 hemicellulosic polymers typical of secondary walls (Voiniciuc *et al.*, 2015c), which are
65 deposited after cells expand.

66 In the past decade, several classes of carbohydrate-active enzymes have been found to
67 influence mucilage content and properties (Griffiths & North, 2017; Šola *et al.*, 2019). At least
68 three genes are required to maintain pectin adherence to the seed surface (Fig. 1a): *CELLULOSE*
69 *SYNTHASE (CESA5)*, *SALT-OVERLY SENSITIVE5 (SOS5)* and *MUCILAGE-*
70 *RELATED21/MUCILAGE-MODIFIED5 (MUCI21/MUM5)*. *CESA5* is a member of the
71 cellulose synthesis complex (Sullivan *et al.*, 2011; Mendu *et al.*, 2011; Harpaz-Saad *et al.*, 2011;
72 Griffiths *et al.*, 2015), while the *SOS5* arabinogalactan protein could be part of a mucilage
73 proteo-glycan or a kinase signalling pathway (Harpaz-Saad *et al.*, 2011; Griffiths *et al.*, 2014;
74 Basu *et al.*, 2016). Although its predicted xylosyltransferase activity remains to be confirmed *in*
75 *vitro* (Voiniciuc *et al.*, 2015a; Zhong *et al.*, 2018), *MUCI21* is required to substitute xylan with
76 xylose branches (Voiniciuc *et al.*, 2015a) that facilitate pectin-cellulose interactions (Ralet *et al.*,
77 2016). Galactoglucomannan, another branched hemicellulose in Arabidopsis mucilage, is
78 elongated by *CSLA* enzymes and substituted by *MANNAN* α -
79 *GALACTOSYLTRANSFERASE1/MUCILAGE-RELATED10 (MAGT1/MUCI10)*; Yu *et al.*,
80 2014, 2018; Voiniciuc *et al.*, 2015b). Unlike xylan, branched HM maintains cellulose deposition
81 and pectin density without appearing to influence mucilage adherence (Fig. 1a).

82 Biochemical and histological analyses of double mutants have clarified how *SOS5* and
83 cellulosic ray-like structures provide two distinct mechanisms to anchor pectin to seeds (Griffiths
84 *et al.*, 2014, 2016; Ben-Tov *et al.*, 2018). The contrasting roles of the two hemicelluloses on
85 mucilage properties have yet to be evaluated in detail. The physiological roles of Arabidopsis
86 seed mucilage are still ambiguous, even though angiosperm seed coats have been involved in
87 seed dormancy, dispersal and germination (Western, 2012; North *et al.*, 2014). In contrast to the
88 Columbia wild type, Arabidopsis varieties with impaired mucilage release (Saez-Aguayo *et al.*,
89 2014) or adherence (Voiniciuc *et al.*, 2015a) have elevated buoyancy and could be dispersed on

90 water. Seed germination is essential for plant establishment and is highly sensitive to salt stress.
91 In this study, we therefore explored how genes affecting different wall polymers modulate
92 mucilage properties, seed germination and early growth under salt stress (Fig. 1a).

93 **Materials and Methods**

94 **Plant materials**

95 Mutations were genotyped using primers listed in Table S1 and Touch-and-Go PCR (Berendzen
96 *et al.*, 2005). The double mutants generated in this study are available from the Nottingham
97 Arabidopsis Stock Center. Plants were grown in climate-controlled chambers as previously
98 described (Voiniciuc *et al.*, 2015b). The germination assays were performed using seeds
99 produced by plants grown individually in 8 cm round pots at 100-120 $\mu\text{E m}^{-2} \text{s}^{-1}$ light, 22°C and
100 around 60% relative humidity. Flowering plants were staked and mature, dry seeds (~10 weeks)
101 were harvested, separated from the chaff and stored in separate paper bags (one per plant) in a
102 temperature-controlled laboratory (~23°C, 40 to 50% humidity).

103 **Microscopic analyses**

104
105 Seeds were stained with 0.01% ruthenium red (RR) in 24-well plates and quantified in Fiji
106 (<https://fiji.sc/>; Schindelin *et al.*, 2012) using established protocols (Voiniciuc *et al.*, 2015b). For
107 staining without shaking, seeds were imbibed in 300 μL of 0.01% RR solution for 15 min.
108 Images were acquired with two stereomicroscope-camera setups: MZ12 with DFC 295, or
109 M165FC with MC170 HD (all from Leica). Mucilage immunolabeling with CCRC-M139
110 (Carbosource, Complex Carbohydrate Research Center) and counter-staining with S4B (Direct
111 Red 23; Sigma Aldrich) was performed using a published protocol and Leica TCS SP8 confocal
112 setup (Voiniciuc, 2017). Germinated seeds were stained with calcofluor white and propidium
113 iodide (0.05%, w/v, for both dyes) for 10 min, rinsed well with water, and imaged on a Zeiss
114 Imager.Z2 with a 10x Plan-Fluar (NA 0.30), Axiocam 506, and DAPI/Texas Red filters.

115 **Biochemical analyses**

116
117 Total mucilage was extracted with a ball mill, hydrolyzed, and quantified via high performance
118 anion exchange chromatography with pulsed amperometric detection (HPAEC-PAD) as
119 previously described (Voiniciuc & Günl, 2016). The quantification of mucilage detachment via
120 HPAEC-PAD has also been described in detail (Voiniciuc, 2016). HPAEC-PAD of mucilage

121 was conducted on a Dionex system equipped with CarboPac PA20 columns (Voiniciuc & Günl,
122 2016). For alcohol-insoluble residue (AIR) isolation, all material (72 h post-stratification) from
123 four biological replicates was pooled, finely ground and sequentially washed with 70% ethanol,
124 chloroform:methanol (1:1, v/v) and acetone. Monosaccharide content of germinated seed AIR
125 after 2 M trifluoroacetic acid hydrolysis was analyzed on a Metrohm 940 Professional IC Vario
126 (Voiniciuc *et al.*, 2019), equipped with Metrosep Carb 2-250/4.0 guard and analytical columns.

127 **Seed germination assay**

128
129 All germination assays were performed in sterile 24-well culture plates (VWR International;
130 734-2779), using 500 μL of the specified solution and dry seeds (typically 20, but up to ~ 100
131 worked) from a single plant per well. The four corners had only water and the plates were sealed
132 with lids and 3M micropore tape to reduce desiccation. Replicates from high-quality seed lots
133 were distributed to avoid positional bias, and at least three biological replicates per genotype
134 showed consistent results. Seeds were hydrated in 500 μL of distilled water, 150 mM CaCl_2 or
135 150 mM NaCl directly in the plate, or first de-mucilaged via ball mill extraction in water
136 (Voiniciuc & Günl, 2016) before rinsing and being transferred in the final solvent (500 μL) to
137 the plates. Floating seeds were counted as the number remaining in the center of each well, atop
138 the solution. Plates were stratified for 66 h (dark, 4°C), transferred to a phytochamber (22°C, 100
139 $\mu\text{E m}^{-2} \text{s}^{-1}$ constant light), and then imaged every 24 h with a Leica M165FC stereomicroscope.
140 Seeds were defined as germinated if radicle length was $>70 \mu\text{m}$, when quantified in Fiji (line
141 tool).

142 To compare ionic and osmotic effects, germination assays were performed in 150 mM
143 CaCl_2 or MgCl_2 salts, 450 mM sorbitol, and 61 mM polyethelene glycol (PEG) 4000, all with an
144 equal osmotic pressure (1.11 MPa) based on the van 't Hoff formula and experimental data
145 (Money, 1989). Radicle protrusion versus elongation effects were tested by switching water and
146 150 mM CaCl_2 at 24 h post-stratification following three sequential 450 μL solvent exchanges.

147

148 **Figures and statistical analysis**

149
150 Micrographs were processed uniformly in Fiji. Numerical data were plotted as bar graphs in
151 Microsoft Excel 365 or as box/violin/jitter plots in the Past 4 statistics software package

152 (<https://folk.uio.no/ohammer/past/>; Hammer *et al.*, 2001)). Panels were assembled in Inkscape
153 (<https://inkscape.org/>). ATH1 microarray expression, including GSE20223 dataset (Narsai *et al.*,
154 2011), was visualized in GENEVESTIGATOR Professional (<https://genevestigator.com/>). Two-
155 samples and multiple samples statistics were performed in Excel and Past 4, respectively.
156 Carbohydrates were drawn according to the Symbol Nomenclature for Glycans (SNFG).

157

158 **Results and Discussion**

159 **Mucilage adherence requires multiple wall polymers, except HM**

160 To dissect the roles of the four genes listed in Fig. 1a, we generated a series of double mutants
161 with defects in HM, xylan, cellulose or an AGP (*SOS5*). We crossed the *muci10-1* (Voiniciuc *et*
162 *al.*, 2015b) and *muci21-1* (Voiniciuc *et al.*, 2015a) hemicellulose mutants to each other, as well
163 as to *cesa5-1* (Mendu *et al.*, 2011) and *sos5-2* (Harpaz-Saad *et al.*, 2011). After shaking and RR
164 staining, the seeds of all single and double mutant combinations had wild-type seed area but
165 were surrounded by smaller mucilage capsules (Fig. 1b,c). *MUCI21*, *CESA5* or *SOS5* were
166 epistatic to *MUCI10* in terms of adherent mucilage size. While all mutants produced wild-type
167 percentages of rhamnose and galacturonic acid in total mucilage extracts (Table S2), significant
168 reductions in minor sugars were associated with *muci10* (galactose and mannose) and *muci21*
169 (xylose) mutations (Fig. 2a). Consistent with previous results (Griffiths *et al.*, 2014), *cesa5* and
170 *sos5* mutations did not alter matrix polysaccharide composition. The *muci10 muci21* double
171 mutant phenocopied the biochemical deficiencies of the respective single mutants, indicating that
172 xylan and HM substitution can be uncoupled in the seed coat.

173 Sequential mucilage extractions (Fig. 2b and Table S3) as well as direct hydration in RR
174 solution (Fig. 2c) showed that more pectin detached from seeds containing *muci21*, *cesa5*, and/or
175 *sos5* mutations compared to wild-type and *muci10*. Xylan detachment increased proportional to
176 that of pectin in mutants lacking *CESA5* and/or *SOS5* (Fig. 2b; Table S3), consistent with
177 covalent linkages between these polymers (Ralet *et al.*, 2016; Voiniciuc *et al.*, 2018).
178 Unbranched xylan epitopes, labelled by the CCRC-M139 monoclonal antibody (Ruprecht *et al.*,
179 2017), closely surrounded *muci21* and *cesa5* seeds, but were further from the surface of *sos5* and
180 other genotypes (Fig. S1a,b), proportional to the RR-stained adherent capsule size (Fig. 1b,c).

181 Each mutation also had distinct effects on S4B staining, which primarily detects cellulose
182 (Anderson *et al.*, 2010), and all the double mutants seeds lacked the ray-like structures that were
183 observed around the wild type (Fig. 2d). Among the single mutants, only *muci21* and *cesa5*
184 displayed clear ray-like structures (Fig. 2d), while *sos5* only had more diffuse cellulose as
185 previously shown (Fig. 2d; Griffiths *et al.*, 2014). The impact of the different mutant
186 combinations on cellulose architecture were also supported by crystalline polymer birefringence
187 (Fig. S1c). In short, *CESA5*, *SOS5*, or *MUCI21* were epistatic to *MUCI10* for pectin adherence
188 (Fig. 2b,c), via partially overlapping mechanisms, and the loss of any two players severely
189 impaired cellulose structure. This double mutant analysis highlights the genetic complexity of
190 cell wall biosynthesis in the seed coat and reveals how extracellular polysaccharide organization
191 can be dramatically reshaped when more than one structural component is modified.

192 **The elongation and substitution of HM modulate salt tolerance**

193 The newly generated mutant collection affecting multiple classes of wall polymers enabled us to
194 investigate the physiological consequences of altering mucilage structure. We established a novel
195 seed germination and salt stress assay using aqueous solutions in 24-well plates. Nearly all wild-
196 type and mutant seeds imbibed in water germinated within 24 h post-stratification (Fig. 3a).
197 However, when placed in 150 mM CaCl₂, few wild-type seeds germinated even after 48 h of
198 exposure to constant light. We initially hypothesized that mucilage-defective mutants might be
199 more susceptible to salt stress, but unexpectedly found that *muci10* and *muci10 muci21* seeds had
200 over 5-fold higher germination rate at this stage (Fig. 3a). The other mutant combinations
201 germinated like the wild type at all time points. Only *muci10* and *muci10 muci21* had
202 significantly longer radicles at 72 h in 150 mM CaCl₂ (Fig. 3b and Fig. 3d), even though most
203 mutants had around a two-fold higher flotation rate compared to the wild type (Fig. 3c). The
204 enhanced germination rate and radicle growth of *muci10* in 150 mM CaCl₂ was replicated in
205 multiple assays, including up to 100 seeds per well and independent growth batches (Fig. 3e-g).

206 To evaluate the basis of the observed salt tolerance, we assayed the effects of the *muci10*
207 mutation in additional stress conditions. The use of 150 mM NaCl also reduced the rate of seed
208 germination, but radicles that protruded from NaCl-treated seeds failed to further elongate
209 compared to the CaCl₂ treatment (Fig. S2). Nevertheless, *muci10* and *muci10 muci21* germinated
210 faster than wild type in both salt treatments (Fig. 3a and Fig. S3a). All seeds sunk in water within
211 the stratification period (Fig. S3b), but a significant proportion of certain seeds (only *muci21* in

212 NaCl, and most mutants in CaCl₂) continued to float in the salt solutions (Fig. S3c). When
213 subjected to ionic (150 mM CaCl₂ or MgCl₂) or purely osmotic stress (PEG 4000 or sorbitol) of
214 equivalent pressure, the germination rate of *muci10* seeds was significantly higher than wild type
215 only in calcium salt stress (Fig. 4a). Once protruded from the seed coat, *muci10* radicles
216 elongated significantly faster than wild type in both CaCl₂ and sorbitol treatments (Fig. 4b;
217 despite 3-fold difference in sample sizes), while the magnesium and PEG solutions showed
218 higher toxicity to both genotypes. Overall, unbranched HM mutant seeds primarily tolerated high
219 amounts of Ca²⁺ cations, which can cross-link unesterified pectin (Voiniciuc *et al.*, 2015c; Šola
220 *et al.*, 2019). Switching water and 150 mM CaCl₂ solutions at 24 h post-stratification
221 demonstrated that *muci10* enhances growth in calcium stress during radicle emergence as well as
222 subsequent elongation (Fig. S3d,e).

223 We then investigated how mucilage removal impacts salt tolerance, by extracting seed coat
224 polysaccharides using a ball mill prior to stratification. With or without mucilage, CaCl₂-treated
225 *muci10* seeds germinated faster than wild-type (Fig. 4c). Mucilage β-glucans continue to
226 encapsulate wild-type seeds at 72 h post-stratification (Fig. 4d), but were absent from de-
227 mucilaged wild-type seeds and from HM-deficient *muci10* seeds (regardless of treatment).
228 Despite not altering the germination rates of after-ripened seeds, the mucilage extraction
229 significantly reduced the radicle length of each genotype compared to the intact controls (Fig.
230 4e). To evaluate the roles of different enzymes involved in HM biosynthesis, we then compared
231 the germination rates of *muci10* and *csla2-3* (Fig. S4), which have similar mucilage defects
232 (Voiniciuc *et al.*, 2015b). CaCl₂-treated *csla2* resembled the wild type, but the mannose content
233 of *csla2* germinated seeds was reduced by only 7% (t-test, P < 0.05) in either water or CaCl₂
234 (Fig. S4c and Table S4), suggesting that additional CSLAs elongate HM in the same tissues.
235 Using microarray data, we found that the transcription of *CSLA2*, *CSLA3*, *CSLA9* along with
236 *CSLA7* and *CSLA11* (to a lesser extent) increased during germination relative to dry seeds (Fig.
237 S4d). Compared to the wild type, we found that the *csla2-1 csla3-2 csla9-1* triple mutant
238 (abbreviated as *csla239*), reported to have glucomannan-deficient stems (Goubet *et al.*, 2009),
239 had significantly lower germination (Fig. 4f) and smaller radicles (Fig. 4g) in the CaCl₂
240 treatment. The *csla239* triple mutant reduced the mannan content of germinated seeds by one-
241 third (Fig. 4h and Table S5), indicating that even a partial reduction of HM elongation
242 significantly impaired growth under salt stress. Since a *csla7* mutant was defective in

243 embryogenesis (Goubet *et al.*, 2003, 2009), we expect that the full disruption of HM elongation
244 in seeds would be lethal.

245 In summary, we found that the biosynthesis of two substituted hemicelluloses in the seed
246 coat epidermis can be uncoupled and that HM and xylan have largely independent functions. HM
247 substituted by MUCI10 is responsible for controlling pectin density, supporting cellulose
248 synthesis and modulating seed tolerance to salt stress. In contrast, *MUCI21*, *CESA5* and *SOS5*
249 are all epistatic to *MUCI10* for pectin adherence to the seed surface, via partially overlapping
250 means (Fig. 1a). Since *muci21*, *cesa5* and *sos5* had additive effects (Fig. 1, Fig. 2, and Fig. S1,
251 *cesa5 sos5* from Griffiths *et al.*, 2014, 2016), Arabidopsis seed mucilage structure must be
252 controlled by a genetic network that is more complex than its carbohydrate composition
253 suggests. For instance, the disruption of HM biosynthesis (Fig. 2; Yu *et al.*, 2014; Voiniciuc *et*
254 *al.*, 2015b) or of cortical microtubule organization (Yang *et al.*, 2019) reduces the distribution of
255 cellulose but not mucilage adherence. Our analysis of *muci10* and *cesa5* single and double
256 mutants indicates that the cellulosic microfibrils essential for pectin attachment might be closer
257 to the seed surface than previously thought (see remnants of rays in Fig. 2d and Fig. S1c).

258 In addition to gaining insight into the genetic regulation of mucilage properties, we
259 discovered that HM structure modulates seed germination in CaCl₂ solutions, and to a lesser
260 extent in other ionic/osmotic conditions. Ca²⁺ ions can cross-link unesterified mucilage pectin
261 and all the generated double mutants had elevated flotation compared to the wild type. However,
262 only the *muci10* mutation promoted germination in CaCl₂, while the *csla239* triple mutant
263 reduced it. Consistent with these effects, *MUCI10* and other HM biosynthetic genes were up-
264 regulated during seed germination (Fig. 1d and Fig. S4d), while *MUCI21* was not. Since *CESA5*
265 was also expressed in germinating seeds (Fig. 1d) and *sos5* roots are overly sensitive to salt (no
266 ATH1 microarray probe; Basu *et al.*, 2016), *muci10 cesa5* and *muci10 sos5* double mutants may
267 offset the benefit of *muci10* (Fig. 3). The presence of unbranched HM could directly alter the
268 ability of cell walls to expand under salt stress. HM deficiencies also modify pectin properties,
269 by lowering the degree of methylesterification (Yu *et al.*, 2014), so *muci10* mucilage might be
270 able to sequester calcium ions that would otherwise inhibit the expansion of inner cell layers.

271 In addition, unsubstituted HM in *muci10* should be more readily hydrolyzed or
272 transglycosylated by β -1,4-mannanases (MAN; Schröder *et al.*, 2009), which are expressed
273 during Arabidopsis seed imbibition (Fig. 1d,e). Mutations in *MAN5*, *MAN7*, and particularly

274 *MAN6* are known to reduce germination in favorable conditions (Iglesias-Fernández *et al.*,
275 2011). We hypothesize that MAN enzymes might directly alter cell wall expansion, mobilize
276 energy reserves and/or release an HM-derived molecular signal to enhance salt tolerance. Only
277 water-treated seedlings accumulated large amounts of glucose (Tables S4 and S5), likely derived
278 from starch. Seeds germinating in salt stress might need to mobilize carbon reserves from HM
279 and potentially other mucilage polymers to sustain growth (Fig. 4). HM structure varies
280 extensively in natural *Arabidopsis* populations (Voiniciuc *et al.*, 2016), so it might already
281 modulate how seeds disperse, germinate and tolerate brackish waters containing hostile levels of
282 Ca^{2+} and/or Na^+ . Consistent with this hypothesis, the constitutive expression of an enzyme
283 involved in producing GDP-mannose, the sugar donor for HM elongation, elevated the mannose
284 content of *Arabidopsis* seedlings and their tolerance to 150 mM NaCl (He *et al.*, 2017). Since the
285 world faces rising sea levels and the expansion of saline environments, engineering salt tolerance
286 remains a major challenge in crop production.

287 In conclusion, we have deciphered the contrasting roles of two classes of hemicelluloses in
288 establishing seed mucilage properties and demonstrated new roles for HM elongation and
289 substitution in radicle emergence as well as elongation during calcium salt stress. The multiwell
290 cultivation system established in this study can be used to explore the physiological
291 consequences of additional cell wall modifications. The overlapping expression profiles of
292 multiple HM-related genes (Fig. 1d and S4d) highlights the need to investigate the specificity of
293 these players on the cellular level in future studies. Future studies using *in vitro* (Liepman *et al.*,
294 2005; Yu *et al.*, 2018) or synthetic biology (Voiniciuc *et al.*, 2019) approaches are required to
295 elucidate the glycan structures yielded by different enzyme isoforms, or combinations thereof.

296

297 **Accession Numbers**

298 MUCI10 (At2g22900); MUCI21 (At3g10320); CESA5 (At5g09870); SOS5 (At3g46550);
299 CSLA2 (At5g22740); CSLA3 (At1g23480); CSLA9 (At5g03760)

300

301 **Acknowledgements**

302 We thank Stefanie Müller, Benita Schmitz and Stefanie Clauß for excellent technical assistance
303 with plant cultivation. We are also grateful to Dr. Debora Gasperini and the Imaging Unit at the
304 Leibniz Institute of Plant Biochemistry for microscope access. The *csla239* triple mutant was

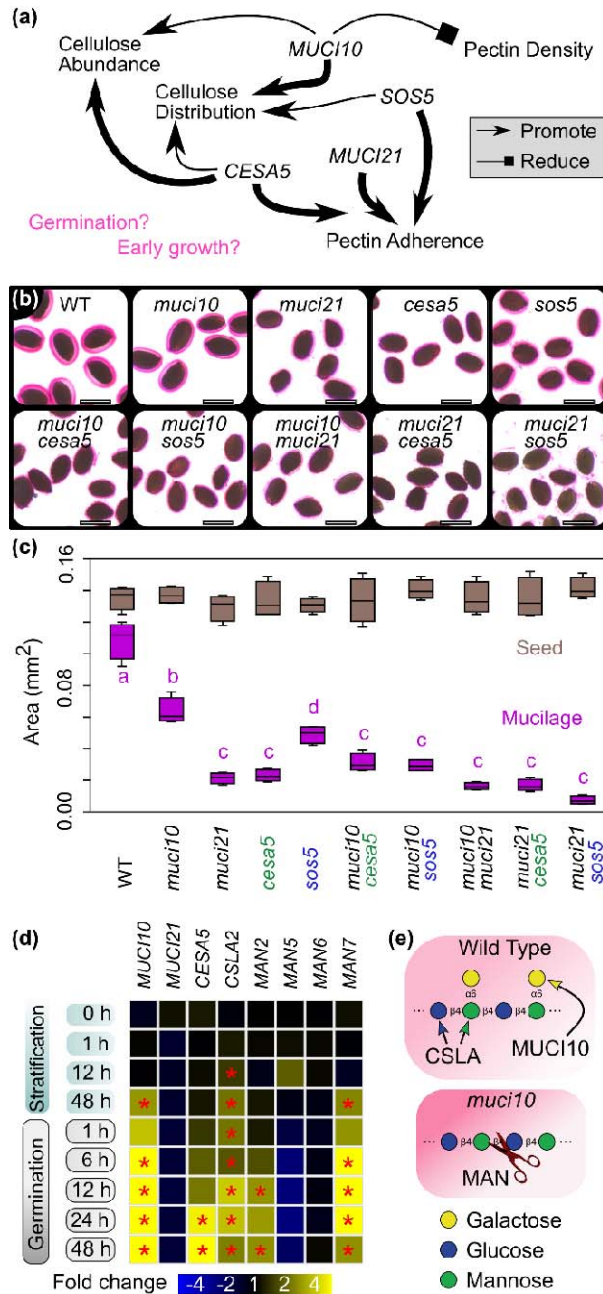
305 kindly provided by Professor Paul Dupree (University of Cambridge). The research was funded
306 in part by the Natural Sciences and Engineering Research Council of Canada (NSERC PGS-D3
307 to C.V.), Deutsche Forschungsgemeinschaft (DFG research grant 414353267 to C.V.; and
308 US98/13-1 to B.U.) and by the Ministry of Innovation, Science and Research of North-Rhine
309 Westphalia within the framework of the NRW Strategieprojekt BioSC (No.
310 313/323□400□00213 to B.U.). Generation of the CCRC series of monoclonal antibodies used in
311 this work was supported by a grant from the NSF Plant Genome Program (DBI-0421683).

312

313 **Author Contributions:**

314 B.Y. and C.V. designed the research. B.U. and C.V. supervised the first and second halves of the
315 project, respectively. B.Y., F.H. and C.V. performed experiments and data analysis. C.V. wrote
316 the article using drafts from B.Y. and valuable feedback from B.U.

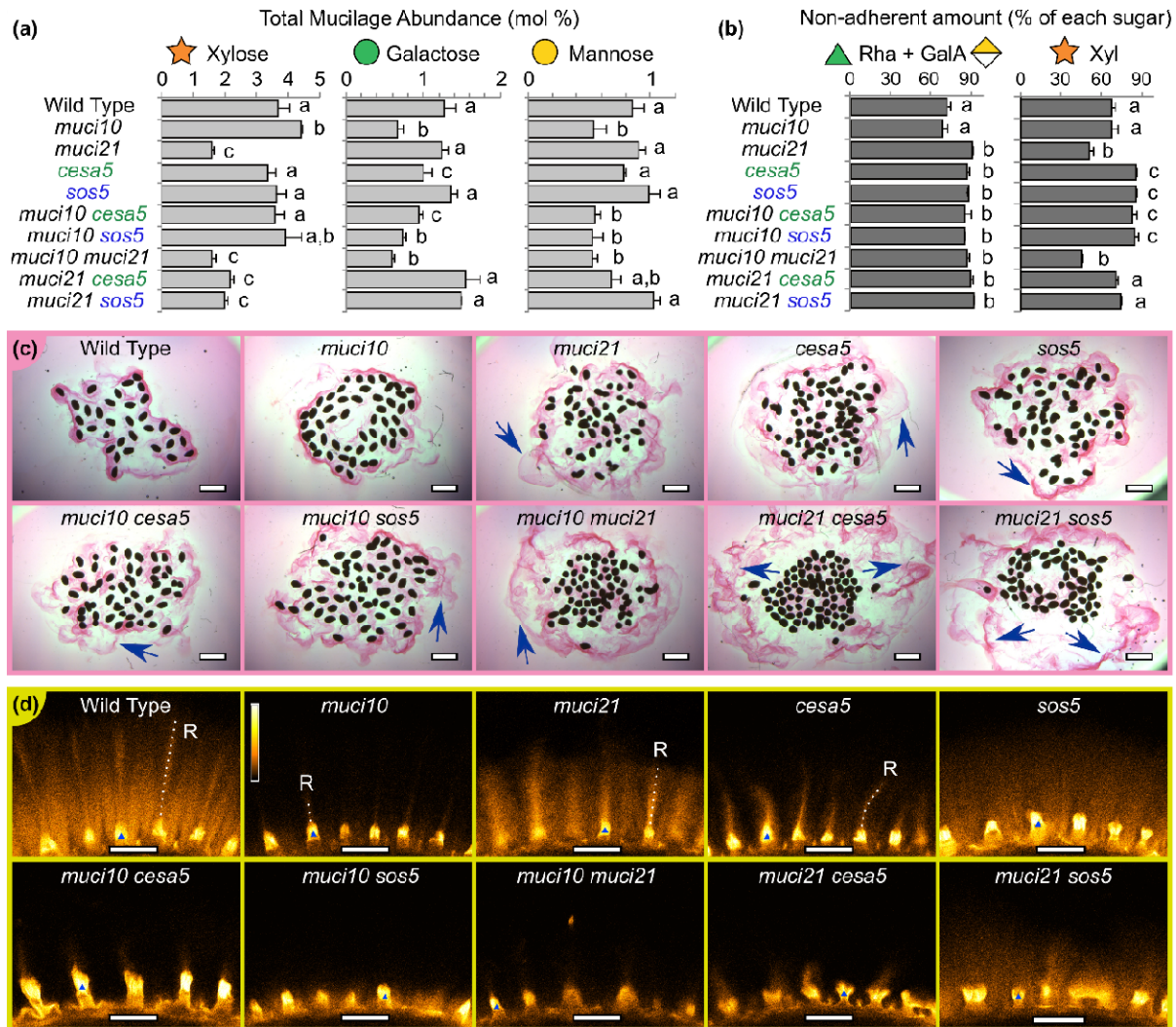
317 **Figures**



318

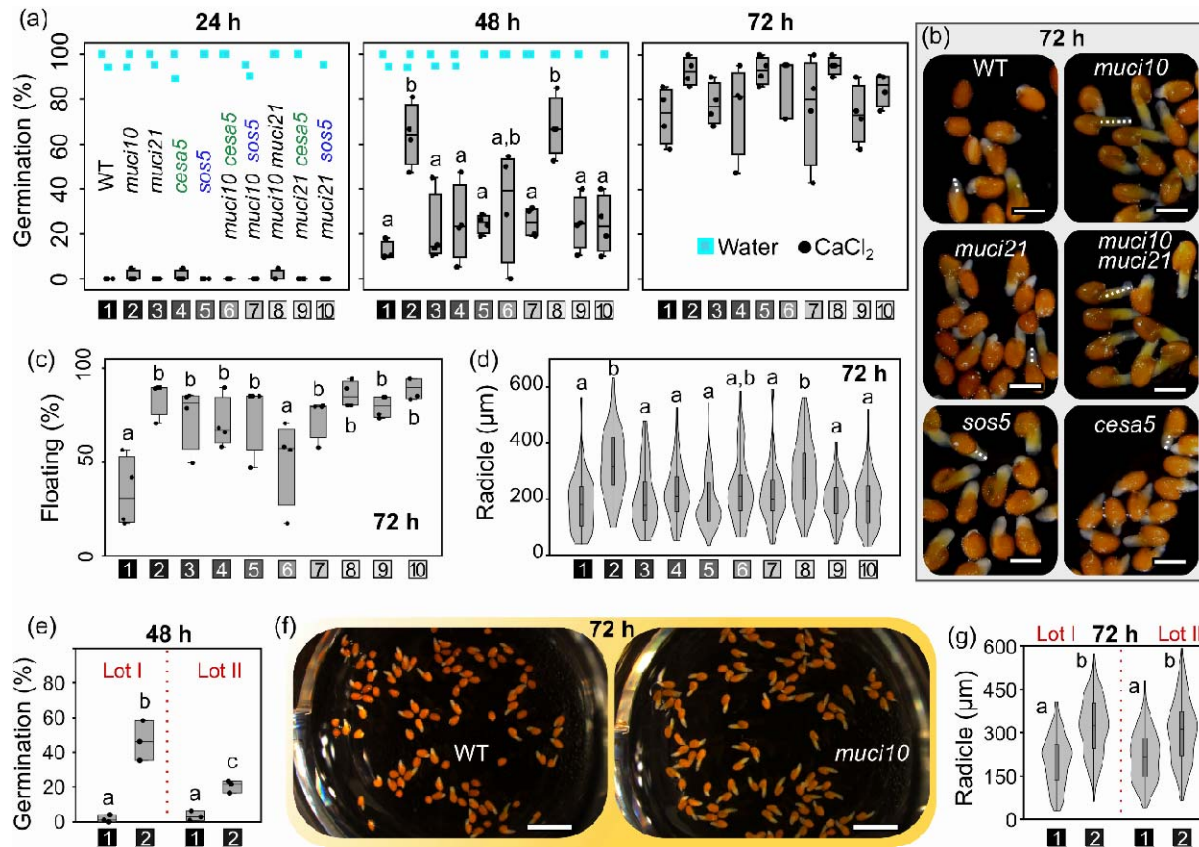
319 **Fig. 1. Impact of different players on mucilage properties.** (a) Schematic of previously
 320 reported functions of four genes on Arabidopsis seed mucilage properties. Genetic interactions
 321 between these players and their physiological roles remain unknown. (b) Wild-type (WT) and
 322 mutant seeds were gently mixed in water and RR was used to stain adherent pectin (pink). Scale
 323 bars = 0.6 mm. (c) Box plots of projected seed and mucilage areas of four biological replicates
 324 (each with around 17 seeds) per genotype. Letters denote significant differences (one-way
 325 ANOVA with Tukey test, P < 0.01). (d) Transcriptional changes (asterisks; P < 0.001) during
 326 stratification and germination relative to dry seeds (0 h), profiled in GENEVESTIGATOR.
 327 (e) Schematic of HM structure in wild-type and *muci10* mutant, which is expected to be more
 328 accessible to cleavage or re-modelling by β -1,4-mannanases (MAN).

329



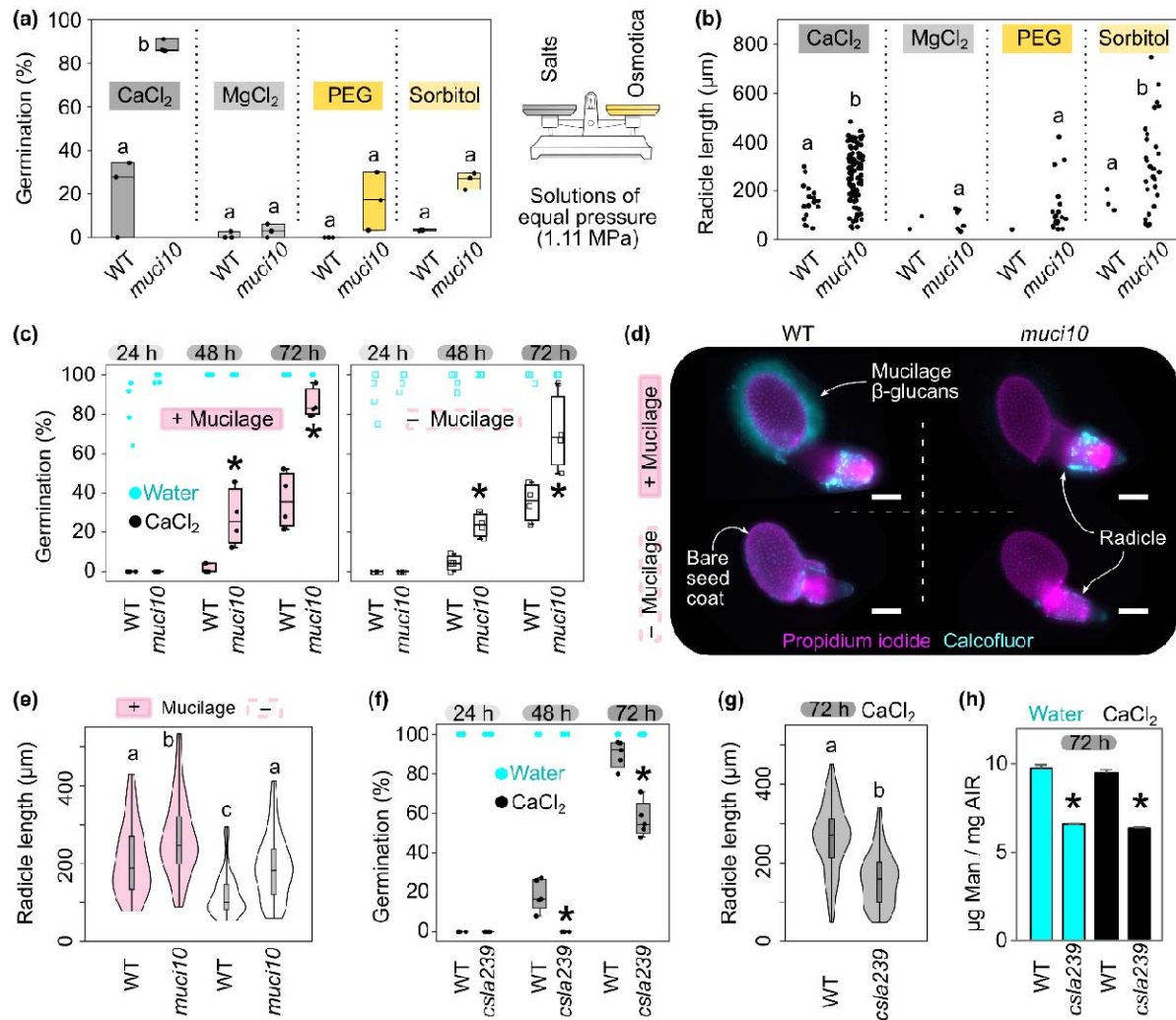
330
 331 **Fig. 2.** Mucilage polysaccharide composition and distribution. (a) Relative abundance of
 332 hemicellulose-derived monosaccharides in total mucilage. (b) The non-adherent proportion of
 333 mucilage pectin (sum of rhamnose and galacturonic acid) and xylan (built of xylose residues).
 334 Data show mean + SD of four biological replicates, except only two for *sos5* in (b), and letters
 335 denote significant differences (one-way ANOVA with Tukey test, $P < 0.05$). (c) Hydration of
 336 seeds in RR solution, without shaking. Blue arrows indicate non-adherent mucilage. (d) S4B
 337 staining of cellulose, coloured using Orange Hot LUT in Fiji (see bar in *muci10* subpanel). Blue
 338 triangles mark volcano-shaped columellae on the seed surface, and the dashed lines indicate
 339 cellulose rays (labelled R). Scale bars = 1 mm (c), 50 μ m (d).

340



341
 342 **Fig. 3.** Germination of seeds in water and CaCl₂. (a) Germination of stratified seeds. Box plots
 343 show germination of single and double mutants (4 plants, ~20 seeds each, per genotype) treated
 344 with 150 mM CaCl₂. In water, nearly all seeds germinated within 24 h. (b) to (d) Further
 345 analyses of seeds from (a) in the CaCl₂ treatment at 72 h. (b) Representative images of
 346 germinated seeds, with dashed lines indicating radicle length. (c) Box plots of seed flotation. (d)
 347 Violin and box plots of the radicle lengths. (e) to (g) Elevated *muci10* tolerance to 150 mM
 348 CaCl₂ stress compared to the wild type (WT) was validated using larger quantities of seeds from
 349 two independent growth batches. (e) Germination rates at 48 h (3 plants, with ~100 seeds each)
 350 per genotype and seed lot. (f) Images of wells from the first seed lot at 72 h. (g) Radicle growth
 351 in CaCl₂ in two seed lots. All X-axes are labeled using the legend in (a), and letters mark
 352 significant changes (one-way ANOVA with Tukey test, P < 0.05). Scale bars = 0.5 mm (b) and 2
 353 mm (f).

354



355

356 **Fig. 4.** Dissecting how HM structure impacts germination in adverse conditions. (a) Germination
 357 rates at 72 h post-stratification in 150 mM CaCl₂, MgCl₂ or two osmotica (PEG 4000 and
 358 sorbitol), with an equal osmotic pressure. (b) Jitter plots showing radicle lengths at 72 h,
 359 from the seeds that germinated in (a). (c) Germination of seeds with (+) or without (-; mill-extracted)
 360 mucilage. (d) Dual cell wall staining of seeds germinated at 72 h in CaCl₂. All *muci10* seeds as
 361 well as mill-extracted wild-type (WT) seeds lack mucilage β-glucans. Scale bars = 200 μm. (e)
 362 Radicle lengths of seeds from (c) at 72 h in CaCl₂. (f) Germination of WT and *csla239* triple
 363 mutant. (g) Radicle length of *csla239* is reduced compared to WT. Data is shown from three
 364 biological replicates in (a) and (b), or four biological replicates in (c) to (g). (h) Mannose content
 365 in germinated seeds shown as mean + SD of two technical replicates. In all panels, significant
 366 changes are marked by different letters (one-way ANOVA with Tukey test, P < 0.05) or asterisks
 367 (student's t-test, P < 0.05; compared to the corresponding WT).

368

369

370

371 **References**

- 372 **Anderson CT, Carroll A, Akhmetova L, Somerville C. 2010.** Real-Time Imaging of Cellulose
373 Reorientation during Cell Wall Expansion in Arabidopsis Roots. *Plant Physiology* **152**: 787–796.
- 374 **Basu D, Tian L, Debrosse T, Poirier E, Emch K, Herock H, Travers A, Showalter AM.**
375 **2016.** Glycosylation of a Fasciclin-Like Arabinogalactan-Protein (SOS5) Mediates Root Growth
376 and Seed Mucilage Adherence via a Cell Wall Receptor-Like Kinase (FEI1/FEI2) Pathway in
377 Arabidopsis. *PLOS ONE* **11**: e0145092.
- 378 **Ben-Tov D, Idan-Molakandov A, Hugger A, Ben-Shlush I, Günl M, Yang B, Usadel B,**
379 **Harpaz-Saad S. 2018.** The role of COBRA-LIKE 2 function, as part of the complex network
380 of interacting pathways regulating Arabidopsis seed mucilage polysaccharide matrix
381 organization. *The Plant Journal* **94**: 497–512.
- 382 **Berendzen K, Searle I, Ravenscroft D, Koncz C, Batschauer A, Coupland G, Somssich IE,**
383 **Ülker B. 2005.** A rapid and versatile combined DNA/RNA extraction protocol and its
384 application to the analysis of a novel DNA marker set polymorphic between Arabidopsis thaliana
385 ecotypes Col-0 and Landsberg erecta. *Plant Methods* **1**: 4.
- 386 **Goubet F, Barton CJ, Mortimer JC, Yu X, Zhang Z, Miles GP, Richens J, Liepman AH,**
387 **Seffen K, Dupree P. 2009.** Cell wall glucomannan in Arabidopsis is synthesised by CSLA
388 glycosyltransferases, and influences the progression of embryogenesis. *The Plant Journal* **60**:
389 527–538.
- 390 **Goubet F, Misrahi A, Park SK, Zhang Z, Twell D, Dupree P. 2003.** AtCSLA7, a Cellulose
391 Synthase-Like Putative Glycosyltransferase, Is Important for Pollen Tube Growth and
392 Embryogenesis in Arabidopsis. *Plant Physiology* **131**: 547–557.
- 393 **Griffiths JS, Crepeau M-J, Ralet M-C, Seifert GJ, North HM. 2016.** Dissecting Seed
394 Mucilage Adherence Mediated by FEI2 and SOS5. *Frontiers in Plant Science* **7**: 1–13.
- 395 **Griffiths JS, North HM. 2017.** Sticking to cellulose: exploiting Arabidopsis seed coat mucilage
396 to understand cellulose biosynthesis and cell wall polysaccharide interactions. *New Phytologist*
397 **214**: 959–966.
- 398 **Griffiths JS, Šola K, Kushwaha R, Lam P, Tateno M, Young R, Voiniciuc C, Dean G,**
399 **Mansfield SD, DeBolt S, et al. 2015.** Unidirectional Movement of Cellulose Synthase
400 Complexes in Arabidopsis Seed Coat Epidermal Cells Deposit Cellulose Involved in Mucilage
401 Extrusion, Adherence, and Ray Formation. *Plant Physiology* **168**: 502–520.

402 **Griffiths JS, Tsai AYL, Xue H, Voiniciuc C, Šola K, Seifert GJ, Mansfield SD, Haughn**
403 **GW. 2014.** SALT-OVERLY SENSITIVE5 mediates arabidopsis seed coat mucilage adherence
404 and organization through pectins. *Plant Physiology* **165**: 991–1004.

405 **Hammer Ø, Harper DAT, Ryan PD. 2001.** PAST: Paleontological statistics software package
406 for education and data analysis. *Palaeontologia Electronica* **4**.

407 **Harpaz-Saad S, McFarlane HE, Xu S, Divi UK, Forward B, Western TL, Kieber JJ. 2011.**
408 Cellulose synthesis via the FEI2 RLK/SOS5 pathway and CELLULOSE SYNTHASE 5 is
409 required for the structure of seed coat mucilage in Arabidopsis. *The Plant Journal* **68**: 941–953.

410 **He C, Yu Z, Teixeira Da Silva JA, Zhang J, Liu X, Wang X, Zhang X, Zeng S, Wu K, Tan**
411 **J, et al. 2017.** DoGMP1 from *Dendrobium officinale* contributes to mannose content of water-
412 soluble polysaccharides and plays a role in salt stress response. *Scientific Reports* **7**: 1–13.

413 **Iglesias-Fernández R, Rodríguez-Gacio MC, Barrero-Sicilia C, Carbonero P, Matilla A.**
414 **2011.** Three endo- β -mannanase genes expressed in the micropylar endosperm and in the radicle
415 influence germination of *Arabidopsis thaliana* seeds. *Planta* **233**: 25–36.

416 **Liepman AH, Wilkerson CG, Keegstra K. 2005.** Expression of cellulose synthase-like (Csl)
417 genes in insect cells reveals that CslA family members encode mannan synthases. *Proceedings of*
418 *the National Academy of Sciences of the United States of America* **102**: 2221–2226.

419 **Mendu V, Griffiths JS, Persson S, Stork J, Downie AB, Voiniciuc C, Haughn GW, DeBolt**
420 **S. 2011.** Subfunctionalization of Cellulose Synthases in Seed Coat Epidermal Cells Mediates
421 Secondary Radial Wall Synthesis and Mucilage Attachment. *Plant Physiology* **157**: 441–453.

422 **Money NP. 1989.** Osmotic Pressure of Aqueous Polyethylene Glycols. *Plant Physiology*.

423 **Narsai R, Law SR, Carrie C, Xu L, Whelan J. 2011.** In-Depth Temporal Transcriptome
424 Profiling Reveals a Crucial Developmental Switch with Roles for RNA Processing and
425 Organelle Metabolism That Are Essential for Germination in Arabidopsis. *Plant Physiology* **157**:
426 1342–1362.

427 **North HM, Berger A, Saez-Aguayo S, Ralet M-C. 2014.** Understanding polysaccharide
428 production and properties using seed coat mutants: future perspectives for the exploitation of
429 natural variants. *Annals of Botany* **114**: 1251–1263.

430 **Ralet M-C, Crépeau M-J, Vigouroux J, Tran J, Berger A, Sallé C, Granier F, Botran L,**
431 **North HM. 2016.** Xylans Provide the Structural Driving Force for Mucilage Adhesion to the
432 *Arabidopsis* Seed Coat. *Plant Physiology* **171**: 165–178.

- 433 **Ruprecht C, Bartetzko MP, Senf D, Dallabernadina P, Boos I, Andersen MCF, Kotake T,**
434 **Knox JP, Hahn MG, Clausen MH, et al. 2017.** A synthetic glycan microarray enables epitope
435 mapping of plant cell wall glycan-directed antibodies. *Plant Physiology* **175**: 1094–1104.
- 436 **Saez-Aguayo S, Rondeau-Mouro C, Macquet A, Kronholm I, Ralet MC, Berger A, Sallé C,**
437 **Poulain D, Granier F, Botran L, et al. 2014.** Local Evolution of Seed Flotation in Arabidopsis.
438 *PLoS Genetics* **10**: 13–15.
- 439 **Schindelin J, Arganda-Carreras I, Frise E, Kaynig V, Longair M, Pietzsch T, Preibisch S,**
440 **Rueden C, Saalfeld S, Schmid B, et al. 2012.** Fiji: an open-source platform for biological-
441 image analysis. *Nature Methods* **9**: 676–682.
- 442 **Schröder R, Atkinson RG, Redgwell RJ. 2009.** Re-interpreting the role of endo- β -mannanases
443 as mannan endotransglycosylase/hydrolases in the plant cell wall. *Annals of Botany* **104**: 197–
444 204.
- 445 **Šola K, Dean GH, Haughn GW. 2019.** Arabidopsis Seed Mucilage: A Specialised Extracellular
446 Matrix that Demonstrates the Structure–Function Versatility of Cell Wall Polysaccharides.
447 *Annual Plant Reviews online* **2**: 1085–1116.
- 448 **Sullivan S, Ralet M-C, Berger A, Diatloff E, Bischoff V, Gonneau M, Marion-Poll A, North**
449 **HM. 2011.** CESA5 Is Required for the Synthesis of Cellulose with a Role in Structuring the
450 Adherent Mucilage of Arabidopsis Seeds. *Plant Physiology* **156**: 1725–1739.
- 451 **Voiniciuc C. 2016.** Quantification of the Mucilage Detachment from Arabidopsis Seeds. *BIO-*
452 *PROTOCOL* **6**: 1–9.
- 453 **Voiniciuc C. 2017.** Whole-seed Immunolabeling of Arabidopsis Mucilage Polysaccharides.
454 *BIO-PROTOCOL* **7**: 1–10.
- 455 **Voiniciuc C, Dama M, Gawenda N, Stritt F, Pauly M. 2019.** Mechanistic insights from plant
456 heteromannan synthesis in yeast. *Proceedings of the National Academy of Sciences* **116**: 522–
457 527.
- 458 **Voiniciuc C, Engle KA, Günl M, Dieluweit S, Schmidt MH-W, Yang J-Y, Moremen KW,**
459 **Mohnen D, Usadel B. 2018.** Identification of Key Enzymes for Pectin Synthesis in Seed
460 Mucilage. *Plant Physiology* **178**: 1045–1064.
- 461 **Voiniciuc C, Günl M. 2016.** Analysis of Monosaccharides in Total Mucilage Extractable from
462 Arabidopsis Seeds. *BIO-PROTOCOL* **6**: 1–12.
- 463 **Voiniciuc C, Günl M, Schmidt MH-W, Usadel B. 2015a.** Highly Branched Xylan Made by

464 IRREGULAR XYLEM14 and MUCILAGE-RELATED21 Links Mucilage to Arabidopsis
465 Seeds. *Plant physiology* **169**: 2481–95.

466 **Voiniciuc C, Schmidt MH-W, Berger A, Yang B, Ebert B, Scheller H V., North HM, Usadel**
467 **B, Günl M. 2015b.** MUCILAGE-RELATED10 Produces Galactoglucomannan That Maintains
468 Pectin and Cellulose Architecture in Arabidopsis Seed Mucilage. *Plant Physiology* **169**: 403–
469 420.

470 **Voiniciuc C, Yang B, Schmidt MH-W, Günl M, Usadel B. 2015c.** Starting to Gel: How
471 Arabidopsis Seed Coat Epidermal Cells Produce Specialized Secondary Cell Walls.
472 *International Journal of Molecular Sciences* **16**: 3452–3473.

473 **Voiniciuc C, Zimmermann E, Schmidt MH-W, Günl M, Fu L, North HM, Usadel B. 2016.**
474 Extensive Natural Variation in Arabidopsis Seed Mucilage Structure. *Frontiers in Plant Science*
475 **7**: 1–14.

476 **Western TL. 2012.** The sticky tale of seed coat mucilages: production, genetics, and role in seed
477 germination and dispersal. *Seed Science Research* **22**: 1–25.

478 **Yang B, Voiniciuc C, Fu L, Dieluweit S, Klose H, Usadel B. 2019.** TRM4 is essential for
479 cellulose deposition in Arabidopsis seed mucilage by maintaining cortical microtubule
480 organization and interacting with CESA3. *New Phytologist* **221**: 881–895.

481 **Yu L, Lyczakowski JJ, Pereira CS, Kotake T, Yu X, Li A, Mogelsvang S, Skaf MS, Dupree**
482 **P. 2018.** The Patterned Structure of Galactoglucomannan Suggests It May Bind to Cellulose in
483 Seed Mucilage. *Plant Physiology* **178**: 1011–1026.

484 **Yu L, Shi D, Li J, Kong Y, Yu Y, Chai G, Hu R, Wang J, Hahn MG, Zhou G. 2014.**
485 CELLULOSE SYNTHASE-LIKE A2, a glucomannan synthase, is involved in maintaining
486 adherent mucilage structure in arabidopsis seed. *Plant Physiology* **164**: 1842–1856.

487 **Zhong R, Cui D, Phillips DR, Ye Z-H. 2018.** A Novel Rice Xylosyltransferase Catalyzes the
488 Addition of 2-O-Xylosyl Side Chains onto the Xylan Backbone. *Plant and Cell Physiology* **59**:
489 554–565.

490
491

492 **Supporting Information**

493

494 Additional Supporting Information is found in the online version of this article

495

496 **Fig. S1** Xylan and crystalline cellulose distribution around seeds.

497 **Fig. S2** Morphology of seeds in CaCl₂ and NaCl treatments.

498 **Fig. S3** Seed germination and flotation rates in water and salt stress.

499 **Fig. S4** Roles of heteromannan-related genes during seed germination.

500 **Table S1** Insertional mutants and genotyping primers used in this study.

501 **Table S2** Monosaccharide composition of total mucilage extracted from seeds.

502 **Table S3** Detachment of mucilage components after gentle shaking.

503 **Table S4** Cell wall composition of *csla2* mutant germinated seeds.

504 **Table S5** Cell wall composition of *muci10* and *csla239* germinated seeds.

